Acta Cryst. (1990). B46, 842–850

Structures of the Local Anaesthetics Ropivacaine and Bupivacaine: Structure Determination and Molecular-Modelling Study

BY HILBERT J. BRUINS SLOT*

CAOS/CAMM Center, University of Nijmegen, Toernooiveld, 6525 ED Nijmegen, The Netherlands

HELMUTH J. BEHM†

Crystallography Laboratory, University of Nijmegen, Toernooiveld, 6525 ED Nijmegen, The Netherlands

AND HANS E. M. KERKKAMP

Institute for Anaesthesiology, University of Nijmegen, Geert Groteplein Zuid 10, 6500 *HB Nijmegen, The Netherlands*

(*Received* 2 *March* 1990; *accepted* 12 *July* 1990)

Abstract

(1) 2-(2,6-Dimethylphenylaminocarbonyl)-1-propylpiperidinium chloride (ropivacaine hydrochloride) monohydrate, $C_{17}H_{27}N_2O^+.Cl^-.H_2O$, $M_r = 328{\cdot}881$, monoclinic, $P2_1$, $a = 9{\cdot}5508$ (14), $b = 7{\cdot}3287$ (6), $c = 13{\cdot}1784$ (7) Å, $\beta = 97{\cdot}429$ (15)°, $V = 914{\cdot}7$ (2) Å^3, $Z = 2$, $D_x = 1{\cdot}194$ g cm^{-3}, λ(Cu $K\alpha$) = 1·54184 Å, $\mu = 19{\cdot}23$ cm^{-1}, $F(000) = 356$, $T = 293$ K, final $R = 0{\cdot}056$ for 2062 observed reflections [$I > 3\sigma(I)$]. (2) 1-Butyl-2-(2,6-dimethylphenylaminocarbonyl)piperidinium chloride (bupivacaine hydrochloride) hemi(ethanol) solvate, $C_{18}H_{29}N_2O^+.Cl^-.0{\cdot}5C_2H_6O$, $M_r = 347{\cdot}927$, monoclinic, $P2_1/n$, $a = 9{\cdot}220$ (3), $b = 11{\cdot}0417$ (17), $c = 20{\cdot}392$ (6) Å, $\beta = 102{\cdot}85$ (4)°, $V = 2024$ (1) Å^3, $Z = 4$, $D_x = 1{\cdot}142$ g cm^{-3}, λ(Cu $K\alpha$) = 1·54184 Å, $\mu = 17{\cdot}43$ cm^{-1}, $F(000) = 756$, $T = 293$ K, final $R = 0{\cdot}064$ for 2318 observed reflections [$I > 3\sigma(I)$]. The structures were solved by Patterson search techniques using a fragment model derived from molecular-mechanics calculations. The conformations of the ropivacaine and bupivacaine cations are very similar. The crystal packing of (1) can be regarded as parallel chains along **b**, consisting of cations hydrogen bonded to water molecules. For (2), the cations are held together by hydrogen bonds to chlorine to form layers parallel to the *101* plane. The disordered ethanol molecules are hydrogen bonded to the chlorine atoms, and are located in the same layers. Extended results from molecular-mechanics and semi-empirical molecular-orbital calculations are compared with those from the X-ray analyses. They show that molecular-mechanics calculations can be used to predict the conformations of both local anaesthetics, whereas the semi-empirical molecular-orbital calculations show less predictive value.

Introduction

Local anaesthetics are chemicals that are widely used in clinical practice and can reversibly block action potentials in excitable membranes. The generation and propagation of action potentials depend on the opening and closing of ionic sodium channels, and usually also of potassium channels, that span these membranes. When sensory nerves are blocked, analgesia is provided, when a motor nerve is blocked, a temporary paralysis is induced.

The present X-ray studies were performed on the active forms of the new (in terms of clinical practice) ropivacaine (the L form) and the (currently most popular) bupivacaine (DL racemic mixture). The results from the X-ray determinations can aid in the explanation of physico-chemical characteristics, such as the lipid solubilities and the protein-binding capacities of these so called amino–amide-type local anaesthetics, but such a discussion is outside the scope of the present article.

Frequently, *a priori* information is used in the X-ray structure determination process. The use of the Cambridge Structural Database (Allen *et al.*, 1979) is widely accepted in this context. The use of molecular-modelling techniques to obtain *a priori* information is limited by the predictive values of these techniques. Therefore, the results of molecular-mechanics and semi-empirical molecular-orbital calculations are compared below with the results from the X-ray determinations, in order to assess their relative predictive values.

* To whom correspondence should be addressed.

† Present address: TTC Microelectronic GMBH, Bahnhoffstrasse 36, D-3060 Stadthagen/Hannover, Federal Republic of Germany.

0108-7681/90/060842-09$03.00

Table 1. *Crystal and experimental data*

	Ropivacaine	Bupivacaine
Structural formula	$C_{17}H_{27}N_2O^+.Cl^-.H_2O$	$C_{18}H_{29}N_2O^+.Cl^-.0{\cdot}5C_2H_6O$
M_r	328·881	347·927
Crystal system	Monoclinic	Monoclinic
Space group	$P2_1$	$P2_1/n$
a (Å)	9·5508 (14)	9·220 (3)
b (Å)	7·3287 (6)	11·0417 (17)
c (Å)	13·1784 (7)	20·392 (6)
β (°)	97·429 (15)	102·85 (4)
V (Å^3)	914·7 (2)	2024 (1)
Z	2	4
D_x (g cm^{-3})	1·194	1·142
Radiation (Å)	λ(Cu $K\alpha$) = 1·54184	λ(Cu $K\alpha$) = 1·54184
μ (cm^{-1})	19·23	17·43
F(000)	355·95	755·89
T(K)	293	293
Crystal dimensions (mm)	0·19 × 0·18 × 0·07	0·48 × 0·22 × 0·18
No. of reflections to determine lattice parameters	25	25
θ range (°)	19–35	20–35
Max. [sin(θ)/λ] (Å^{-1})	0·588	0·609
hkl range		
h	−11, 11	−11, 11
k	−8, 8	0,13
l	−15, 15	−24, 24
No. of standard reflections	3	3
Drift correction range	1·031–0·981	1·120–0·989
Empirical absorption correction range	1·000–0·897	0·999–0·894
Total data measured	6206	8082
Unique data	1688	3827
$R_{int} = \Sigma(I - \langle I\rangle)/\Sigma I$	0·023	0·017
Data used in refinement	2062	2318
Parameters refined	189	244
R	0·056	0·064
$wR[w^{-1} = \sigma^2(F) + gF^2]$	0·053	0·069
S	0·294	2·805
Weighting-scheme parameter g	0·001	0·004
Max. shift/e.s.d. in last cycle	0·015	0·084
Final difference Fourier map peaks (e Å^{-3})		
Min.	−0·27	−0·30
Max.	0·23	0·45

X-ray structure determinations

Experimental

Ropivacaine (1) and bupivacaine (2) were supplied by Astra Alab, Sodertalje, Sweden. An enantiomerically pure salt was only provided for (1). Recrystallization from 1:1 ethanol/water (1) and from 1:1 ethanol/acetone (2) yielded needle-shaped crystals. Data sets were collected on an Enraf–Nonius CAD-4 diffractometer using graphite-monochromatized Cu $K\alpha$ radiation (λ = 1·54184 Å) with the ω–2θ scan technique ($0 < \theta < 70°$), a scan angle of 1·5° and a variable scan rate with a maximum scan time of 20 s per reflection. Profile analysis was performed on all reflections (Lehman & Larsen, 1974; Grant & Gabe, 1978). Normal Lorentz–polarization corrections and empirical absorption corrections using ψ scans (North, Phillips & Mathews, 1968) were applied. Crystal and experimental data are summarized in Table 1.

As opposed to the straightforward data collection for (2), the crystals of (1) appeared to be twinned. From CAD-4 data collected to determine the unit cell dimensions, it appeared that the two indiviuals (i and ii) of the crystal share their *ab* plane. The twinning operation is the reflection in this *ab* plane. The resulting angle between $\mathbf{a}_i^*$ and $\mathbf{a}_{ii}^*$ is 165·14 (2)°. Fig. 1 shows the *h*0*l* zone, in which indices for both lattices are given. Reflections with $h = 0$ coincide for the two lattices. Again, there is a hypothetical coincidence for $h = 2{\cdot}8$, therefore the reflections $3n,k,l$ were excluded from the least-squares refinement. The structures were solved using the automated Patterson search methods of the *DIRDIF* system (Beurskens *et al.*, 1984; Beurskens, Gould, Bruins Slot & Bosman, 1987).

For the orientation and translation searches the non-hydrogen fragment (I) was used. Coordinates for this fragment were obtained from molecular-mechanics calculations using *MacroModel* (Mohamadi *et al.*, 1990; see later section on *Molecular modelling*). In the *DIRDIF* Fourier synthesis, all non-H atoms were found for both (1) and (2). The structures were refined isotropically. The phenyl groups were treated as regular hexagons, with C—C distances of 1·395 Å. During the isotropic refinement, a peak in the difference Fourier map was assigned as water oxygen [O(2)] for ropivacaine, and three peaks in the difference Fourier map of bupivacaine were assigned C(19) with full occupancy, and C(20) and O(21) with half occupancy, to form disordered acetone. H atoms were located from subsequent difference Fourier maps and their positions were refined together with fixed isotropic temperature factors taken from the relevant bonded non-H atom. Except for the H atoms bonded to N, the H atoms were refined using a riding model. No positional parameters could be obtained for the amino proton H(2) in ropivacaine: isotropic refinement of H(2), placed at a calculated position using the riding

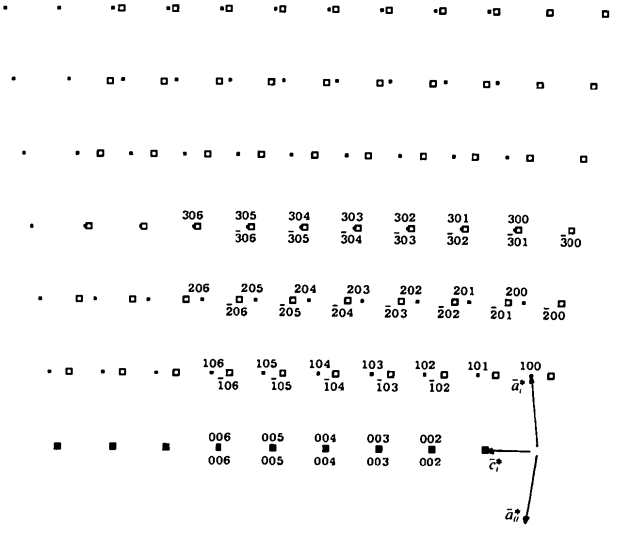

Fig. 1. Indexed *h*0*l* zone of ropivacaine. Individual *i* are denoted by points with indices given above; individual *ii* are denoted by open squares with indices given below.

model, resulted in an unacceptably large temperature factor. H atoms could not be located for the solvent molecules in either structure. After an additional empirical absorption correction using *DIFABS* (Walker & Stewart, 1983), the non-H atoms were refined anisotropically, except for the solvent molecules which were refined isotropically. An examination of the temperature factors of the atoms C(19), C(20) and O(21) now revealed that the initial solvent assignment was incorrect. A description as disordered ethanol with occupancies of 1·0, 0·25 and 0·25 for the renamed atoms C(19), O(20) and O(21) respectively, was more appropriate than disordered acetone. Isotropic refinement of this model with fixed site-occupancy factors showed a consistent set of temperature factors. The H atoms of the methyl groups in (2) appeared to be disordered and a difference Fourier map yielded alternative positions. Positional parameters, site-occupancy factors and fixed isotropic temperature factors were refined for all methyl H atoms using distance constraints. *SHELX* (Sheldrick, 1976) was used for the refinements and as a source of atomic scattering factors. The absolute configuration of (1) was confirmed using *BIJVOET* (Beurskens, Noordik & Beurskens, 1980), $B = 0.9933$ (3). Positional parameters for all non-H atoms are given in Table 2 for both (1) and (2).*

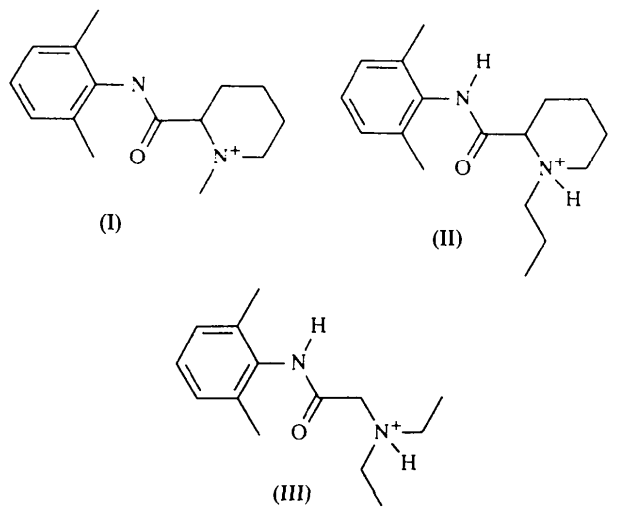

Table 2. *Atomic coordinates with site-occupancy factors and equivalent isotropic temperature factors* (Å²) *for ropivacaine and bupivacaine*

The first line gives values for ropivacaine, the second for bupivacaine. $U_{eq} = (1/3)\sum_i \sum_j U_{ij} a_i^* a_j^* \mathbf{a}_i . \mathbf{a}_j$.

	x	y	z	S.o.f.	U_{eq}/U_{iso}
N(1)	−0·7671 (4)	0·0996 (5)	−0·3652 (3)	1	0·0451 (13)
	0·7305 (4)	0·0228 (3)	0·6344 (2)	1	0·0543 (11)
N(2)	−0·8471 (3)	−0·0841 (4)	−0·1261 (2)	1	0·0354 (9)
	0·6978 (3)	0·0098 (3)	0·8056 (2)	1	0·0507 (11)
O(1)	−0·7853 (4)	−0·1960 (4)	−0·3215 (2)	1	0·0570 (12)
	0·7078 (3)	0·1767 (2)	0·7052 (1)	1	0·0638 (11)
C(1)	−0·7769 (3)	0·0723 (5)	−0·4723 (1)	1	0·0434 (13)
	0·7074 (3)	0·0942 (2)	0·5758 (1)	1	0·0565 (13)
C(2)	−0·6559 (3)	0·0803 (5)	−0·5211 (1)	1	0·0565 (15)
	0·8278 (3)	0·1207 (2)	0·5472 (1)	1	0·0668 (16)
C(3)	−0·6665 (3)	0·0604 (5)	−0·6271 (1)	1	0·0689 (19)
	0·8062 (3)	0·1883 (2)	0·4880 (1)	1	0·0858 (22)
C(4)	−0·7982 (3)	0·0324 (5)	−0·6842 (1)	1	0·0681 (19)
	0·6642 (3)	0·2294 (2)	0·4574 (1)	1	0·0928 (24)
C(5)	−0·9192 (3)	0·0244 (5)	−0·6354 (1)	1	0·0575 (15)
	0·5438 (3)	0·2029 (2)	0·4860 (1)	1	0·0809 (21)
C(6)	−0·9086 (3)	0·0444 (5)	−0·5294 (1)	1	0·0493 (14)
	0·5654 (3)	0·1353 (2)	0·5452 (1)	1	0·0655 (17)
C(7)	−0·5115 (6)	0·1043 (10)	−0·4575 (4)	1	0·0784 (23)
	0·9807 (5)	0·0784 (5)	0·5806 (3)	1	0·0881 (22)
C(8)	−1·0417 (5)	0·0410 (6)	−0·4769 (4)	1	0·0575 (19)
	0·4332 (5)	0·1084 (4)	0·5746 (2)	1	0·0805 (18)
C(9)	−0·7721 (4)	−0·0338 (5)	−0·2981 (3)	1	0·0410 (12)
	0·7346 (4)	0·0690 (3)	0·6947 (2)	1	0·0495 (12)
C(10)	−0·7537 (4)	0·0268 (5)	−0·1854 (3)	1	0·0353 (12)
	0·7859 (3)	−0·0159 (3)	0·7541 (2)	1	0·0497 (12)
C(11)	−0·5999 (4)	−0·0011 (8)	−0·1399 (3)	1	0·0469 (12)
	0·9508 (4)	0·0095 (4)	0·7835 (2)	1	0·0703 (16)
C(12)	−0·5779 (4)	0·0598 (6)	−0·0277 (3)	1	0·0522 (14)
	1·0094 (5)	−0·0590 (4)	0·8484 (2)	1	0·0790 (18)
C(13)	−0·6786 (4)	−0·0422 (6)	0·0314 (3)	1	0·0487 (14)
	0·9164 (5)	−0·0310 (4)	0·8978 (2)	1	0·0793 (18)
C(14)	−0·8302 (4)	−0·0186 (6)	−0·0163 (3)	1	0·0438 (12)
	0·7544 (5)	−0·0602 (3)	0·8692 (2)	1	0·0646 (16)
C(15)	−1·0020 (4)	−0·0904 (6)	−0·1705 (3)	1	0·0429 (13)
	0·5327 (4)	−0·0040 (3)	0·7799 (2)	1	0·0623 (14)
C(16)	−1·0759 (6)	0·0893 (7)	−0·1854 (4)	1	0·0534 (16)
	0·4785 (4)	−0·1298 (4)	0·7617 (3)	1	0·0811 (19)
C(17)	−1·2303 (5)	0·0571 (8)	−0·2247 (4)	1	0·0697 (17)
	0·3110 (5)	−0·1304 (5)	0·7367 (3)	1	0·0982 (21)
C(18)	–	–	–	–	–
	0·2403 (6)	−0·2511 (5)	0·7314 (3)	1	0·1202 (30)
Cl(1)	−0·8230 (1)	−0·5000	−0·0817 (1)	1	0·0509 (3)
	0·8372 (1)	−0·2487 (1)	0·6220 (1)	1	0·0757 (4)
O(2)	−0·6746 (4)	−0·5502 (4)	−0·2763 (3)	1	0·0663 (13)
	–	–	–	–	–
C(19)	–	–	–	–	–
	0·4381 (8)	−0·0234 (8)	0·9736 (4)	1	0·149 (3)
O(20)	–	–	–	–	–
	0·4235 (16)	0·0564 (15)	0·9191 (8)	0·25	0·113 (5)
O(21)	–	–	–	–	–
	0·3219 (20)	−0·0895 (17)	0·9851 (9)	0·25	0·137 (6)

Discussion of the X-ray structures

Plots of the numbering schemes used for both (1) and (2) are shown in Fig. 2. Selected bond lengths, valence angles and torsion angles, obtained using *PARST* (Nardelli, 1983), are given in Table 3. No anomalous geometric values are observed.

It is of interest to compare the molecular conformations of the local anaesthetics with the closely

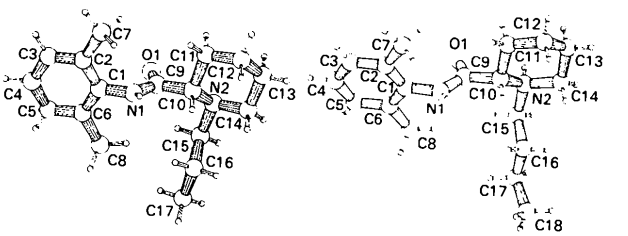

Fig. 2. Perspective drawings of ropivacaine (left) and bupivacaine (right).

* Lists of structure factors, positional and (an)isotropic thermal parameters, bond lengths, angles and torsion angles have been deposited with the British Library Document Supply Centre as Supplementary Publication No. SUP 53362 (69 pp.). Copies may be obtained through The Technical Editor, International Union of Crystallography, 5 Abbey Square, Chester CH1 2HU, England.

Table 3. *Bond lengths* (Å), *bond angles* (°) *and torsion angles* (°) *for non*-H *atoms of ropivacaine* (1) *and bupivacaine* (2)

	(1)	(2)
C(1)—C(2)	1·395 (4)	1·394 (4)
C(1)—C(6)	1·395 (4)	1·395 (4)
C(1)—N(1)	1·416 (4)	1·409 (4)
C(2)—C(3)	1·395 (2)	1·395 (3)
C(2)—C(7)	1·529 (6)	1·498 (5)
C(3)—C(4)	1·395 (4)	1·395 (4)
C(4)—C(5)	1·395 (4)	1·395 (4)
C(5)—C(6)	1·395 (2)	1·395 (3)
C(6)—C(8)	1·524 (6)	1·503 (6)
C(9)—C(10)	1·538 (5)	1·521 (5)
C(9)—O(1)	1·230 (5)	1·243 (4)
N(1)—C(9)	1·323 (5)	1·324 (5)
N(2)—C(15)	1·520 (5)	1·503 (5)
C(10)—C(11)	1·527 (5)	1·531 (5)
C(10)—N(2)	1·499 (5)	1·491 (5)
C(11)—C(12)	1·533 (6)	1·516 (6)
C(12)—C(13)	1·511 (6)	1·494 (7)
C(13)—C(14)	1·511 (6)	1·513 (6)
C(14)—N(2)	1·513 (5)	1·500 (5)
C(15)—C(16)	1·495 (7)	1·495 (5)
C(16)—C(17)	1·517 (7)	1·515 (6)
C(17)—C(18)	–	1·477 (7)
C(1)—C(2)—C(3)	120·0 (2)	120·0 (3)
C(1)—C(2)—C(7)	119·6 (3)	120·0 (3)
C(1)—C(6)—C(5)	120·0 (2)	120·0 (3)
C(1)—C(6)—C(8)	120·3 (2)	121·4 (3)
C(1)—N(1)—C(9)	123·9 (3)	122·8 (3)
C(2)—C(1)—C(6)	120·0 (2)	120·0 (2)
C(2)—C(1)—N(1)	120·1 (3)	119·2 (3)
C(2)—C(3)—C(4)	119·9 (2)	120·0 (3)
C(3)—C(2)—C(7)	120·3 (3)	120·0 (3)
C(3)—C(4)—C(5)	120·0 (1)	120·0 (2)
C(4)—C(5)—C(6)	120·0 (2)	120·0 (3)
C(5)—C(6)—C(8)	119·7 (2)	118·6 (3)
C(6)—C(1)—N(1)	119·8 (3)	120·7 (3)
C(9)—C(10)—C(11)	108·9 (3)	107·7 (3)
C(9)—C(10)—N(2)	110·2 (3)	108·7 (3)
N(1)—C(9)—C(10)	115·0 (3)	116·2 (3)
N(1)—C(9)—O(1)	123·9 (4)	124·2 (3)
N(2)—C(15)—C(16)	116·2 (4)	115·9 (3)
O(1)—C(9)—C(10)	121·1 (3)	119·5 (3)
C(10)—C(11)—C(12)	110·2 (3)	112·4 (3)
C(10)—N(2)—C(14)	109·2 (3)	111·8 (3)
C(10)—N(2)—C(15)	115·5 (3)	113·8 (3)
C(11)—C(10)—N(2)	109·2 (3)	109·8 (3)
C(11)—C(12)—C(13)	109·7 (4)	109·8 (4)
C(12)—C(13)—C(14)	111·6 (3)	111·2 (4)
C(13)—C(14) N(2)	109·9 (3)	110·4 (3)
C(14)—N(2)—C(15)	110·9 (3)	112·3 (3)
C(15)—C(16)—C(17)	109·2 (4)	110·3 (4)
C(16)—C(17)—C(18)	–	115·4 (4)
C(1)—C(2)—C(3)—C(4)	0·0 (4)	0·0 (4)
C(1)—N(1)—C(9)—C(10)	177·8 (3)	−170·1 (3)
C(1)—N(1)—C(9)—O(1)	0·2 (6)	5·6 (6)
C(10)—C(11)—C(12)—C(13)	56·3 (5)	−55·2 (5)
C(10)—N(2)—C(15)—C(16)	−57·5 (5)	66·8 (4)
C(11)—C(10)—N(2)—C(14)	61·9 (4)	−55·6 (4)
C(11)—C(10)—N(2)—C(15)	−172·3 (3)	175·9 (3)
C(11)—C(12)—C(13)—C(14)	−55·5 (5)	56·6 (5)
C(12)—C(13)—C(14)—N(2)	57·9 (4)	−58·2 (5)
C(13)—C(14)—N(2)—C(10)	−60·7 (4)	57·9 (4)
C(13)—C(14)—N(2)—C(15)	170·9 (3)	−172·8 (3)
C(14)—N(2)—C(15)—C(16)	67·4 (5)	−61·5 (4)
C(15)—C(16)—C(17)—C(18)	–	−167·0 (4)
C(2)—C(1)—C(6)—C(5)	0·1 (4)	0·1 (4)
C(2)—C(1)—C(6)—C(8)	−178·2 (3)	180·0 (3)
C(2)—C(1)—N(1)—C(9)	−103·1 (4)	104·3 (4)
C(2)—C(3)—C(4)—C(5)	0·0 (4)	0·0 (4)
C(3)—C(4)—C(5)—C(6)	0·0 (4)	0·0 (4)
C(4)—C(5)—C(6)—C(1)	0·0 (4)	0·0 (4)
C(4)—C(5)—C(6)—C(8)	178·2 (3)	180·0 (3)
C(6)—C(1)—C(2)—C(3)	0·0 (4)	−0·1 (4)
C(6)—C(1)—C(2)—C(7)	−177·9 (4)	178·9 (3)
C(6)—C(1)—N(1)—C(9)	79·4 (5)	−77·4 (4)
C(7)—C(2)—C(3)—C(4)	177·9 (4)	−179·0 (3)
C(9)—C(10)—C(11)—C(12)	179·5 (3)	172·8 (3)
C(9)—C(10)—N(2)—C(14)	−178·5 (3)	−173·2 (3)
C(9)—C(10)—N(2)—C(15)	−52·7 (4)	58·3 (4)
N(1)—C(1)—C(2)—C(3)	−177·5 (3)	178·2 (3)
N(1)—C(1)—C(2)—C(7)	4·6 (5)	−2·8 (4)
N(1)—C(1)—C(6)—C(5)	177·6 (3)	−178·2 (2)

Table 3 (*cont.*)

	(1)	(2)
N(1)—C(1)—C(6)—C(8)	−0·7 (5)	1·8 (4)
N(1)—C(9)—C(10)—C(11)	−97·3 (4)	98·1 (4)
N(1)—C(9)—C(10)—N(2)	142·9 (3)	−143·0 (3)
N(2)—C(10)—C(11)—C(12)	−60·1 (4)	54·6 (4)
N(2)—C(15)—C(16)—C(17)	−177·0 (4)	−179·9 (4)
O(1)—C(9)—C(10)—C(11)	80·3 (5)	−77·8 (4)
O(1)—C(9)—C(10)—N(2)	−39·5 (5)	41·1 (4)

related lidocaine derivatives [(II) and (III) depict the active forms of ropivacaine and lidocaine respectively]. The related compounds were found using a connectivity search on the Cambridge Structural Database (CSD) (Allen *et al.*, 1979) using 2,6-acetoxylidide as search fragment. This search gave seven structures with nine unique fragments. CSD reference codes for the seven structures are: BEFLUT (Faggiani, Lock, Deutsch, Richards & Srivastava, 1982), BEVMOE (Głowka & Gałdecki, 1981), LIDCAN10 (Hanson & Banner, 1974), LIDNPP (Yoo, Abola, Wood, Sax & Pletcher, 1975), LIDOCA10 (Hanson, 1972), LIDOCN (Hanson & Rohrl, 1972) and LIPFAZ (Germain, Declercq, van Meerssche & Koch, 1977). The fragments are characterized by two planar groups: the 'phenyl group' consisting of the atoms C(1) to C(8) and N(1), and the 'amide group' consisting of the atoms C(1), N(1), C(9), O(1), C(10) (average deviations from least-squares planes in the retrieved entries vary from 0·002 to 0·034 Å). The angles between the phenyl groups and amide groups are given in Table 4. Further, to extend the comparison of lidocaine derivatives presented by Yoo *et al.*, the conformation along the main chain [*i.e.* C(1)—N(1)—C(9)—C(10)—N(2)] is also given in Table 4, together with relevant crystallographic characteristics of the structures extracted from the CSD. In order to compare these structures correctly, it was necessary to generate symmetry-related (inverted) fragments for bupivacaine, BEFLUT, and one of the unique fragments from each of BEVMOE and LIDOCA10. Inclusion of the main-chain conformation for LIPFAZ is questionable since the space-group symmetry prohibits inversion. However, results from the inverted structure of LIPFAZ were added to Table 4 because the resemblance of this conformation to the conformation of ropivacaine is striking. This comparison indicates that the structure of LIPFAZ as published by Germain *et al.* should probably be inverted. Yoo *et al.* (1975) reported a different main-chain conformation for LIDOCA10 compared with LIDNPP and LIDOCN. Ropivacaine and bupivacaine resemble the conformation of LIDOCA10. Also, from the structures extracted from the CSD, the conformations of the main chain of BEFLUT, of one of the independent molecules of BEVMOE and of LIPFAZ can be regarded as belonging to this same group. A totally different conformation is

Table 4. *Conformational comparison of ropivacaine and bupivacaine with selected related compounds*

Name[a]	Space group	R	Angle[d]	$T11$[e]	$T12$	$T21$	$T22$	$T31$	$T32$	$T41$	$T42$	H bond[f]
Ropivacaine[b]	$P2_1$[c]	0·056	78·4	−103·1	79·4	0·2	177·8	142·9	−39·5	−178·5	−52·7	1
Bupivacaine[b]	$P2_1/n$	0·064	71·9	−104·3	77·4	−5·6	170·1	143·0	−41·1	173·2	−58·3	1
BEFLUT	$P2_1/c$	0·043	82·6	−98·6	82·3	0·7	−179·8	157·0	−23·5	168·6	−68·3	–
BEVMOE1[b]	$P2_1/c$	0·114	88·8	−89·4	93·4	0·4	177·8	143·6	−39·0	168·1	−63·9	1
LIDOCA10[b]	$C2/c$	0·044	65·5	−111·1	70·1	−5·6	173·3	168·0	−13·0	153·4	−78·1	1
LIPFAZ	$P2_12_12_1$	0·090	71·4	−73·5	106·9	4·4	−179·2	141·9	−41·9	170·0	−66·1	–
LIDNPP[b]	$P2_1/c$	0·067	62·4	−113·6	67·9	−6·2	172·2	149·7	−31·8	79·0	−50·4	–
LIDOCN	$P2_1/c$	0·110	71·9	−105·6	76·9	−4·9	173·8	131·5	−49·8	72·9	−57·0	–
LIDCAN101	$P2_1/c$	0·110	76·3	−80·7	102·9	5·1	−177·1	5·2	−177·0	−128·8	107·0	2
LIDCAN102	$P2_1/c$	0·110	82·1	−82·4	98·3	0·0	−179·4	−1·8	178·8	−131·1	115·9	2
BEVMOE2[b]	$P2_1/c$	0·114	80·8	−101·0	79·0	3·5	−177·7	168·8	−12·4	−123·5	118·5	1

Notes: (*a*) for references to structures, see text; (*b*) protonated at N(2); (*c*) absolute configuration determined; (*d*) angle (°) between least-squares plane through C(1) to C(8) and N(1) and least-squares plane through C(1), N(1), C(9), O(1) and C(10); (*e*) torsion angles Tij (°) according to Klyne & Prelog (1960), $T11$ = C(2)—C(1)—N(1)—C(9), $T12$ = C(6)—C(1)—N(1)—C(9), $T21$ = C(1)—N(1)—C(9)—O(1), $T22$ = C(1)—N(1)—C(9)—C(10), $T31$ = N(1)—C(9)—C(10)—N(2), $T32$ = O(1)—C(9)—C(10)—N(2), $T41$ = C(9)—C(10)—N(2)—C(14), $T42$ = C(9)—C(10)—N(2)—C(15); (*f*) intramolecular hydrogen bond between (1) N(2)—H···O(1), (2) N(1)—H···N(2).

found for both molecules in LIDCAN10, where the intramolecular N(1)—H···N(2) hydrogen bond has a crucial influence. The conformation of the main chain of the other independent moiety in BEVMOE is different from all of the others. It should be noted that intermolecular hydrogen bonds play a role in the conformation of the main chain. For the conformations listed in Table 4, all N(1) atoms act as intermolecular hydrogen-bond donors, as do the protonated N(2) atoms. For the entries in which the N(2) atoms are not protonated (BEFLUT, LIPFAZ, LIDOCN and LIDCAN10), N(2) atoms do not take part in intermolecular hydrogen bonding as acceptors. For the amide O(1) atoms, intermolecular hydrogen bonds are found for the entries BEVMOE (for only one independent molecule), LIDOCA10, LIDOCN and both independent molecules of LIDCAN10, and ropivacaine.

Although the conformations of the ropivacaine (1) and bupivacaine (2) cations are very similar (for a least-squares fit of all common non-H atoms, see Fig. 3; mean deviation = 0·22 Å), the molecular packing arrangements are quite different. In (1), adjacent cations are joined by strong hydrogen bonds to water, *i.e.* between O(1)···H—O(2) and O(2)···H(1′)—N(1′), to form chains parallel to **b**. Also, the chloride anion participates in hydrogen bonding by accepting a water proton and an amino proton. (The amino proton could not be located, but distances and angles involved in the assumed hydrogen-bonding scheme are acceptable.) The rather weak intramolecular hydrogen bond between O(1) and N(2) as described by Hanson (1972) is less favourable than the N(2)···Cl(1) hydrogen bond. Table 5 summarizes the distances and angles involved in hydrogen bonding. Fig. 4 shows the packing perpendicular to the *bc* plane for (1). Fig. 5 shows a perspective drawing of the crystal packing perpendicular to the *bc* plane for (2) [Figs. 2, 4 and 5 were created using *PLUTON* from the *EUCLID* package (Spek, 1982)]. Bupivacaine cations, chlorine anions and the disordered ethanol molecules are held together by hydrogen bonds and van der Waals contacts to form layers parallel to the (101) plane. All positions of the disordered ethanol are shown to illustrate the connectivity in the total hydrogen-bonding scheme. As in (1), the hydrogen bond between Cl(1) and N(2) is stronger than the intramolecular hydrogen bond between O(1) and N(2), because of the unfavourable angles involved in the latter. Table 5 summarizes the hydrogen-bonding scheme in terms of distances and angles. The layers perpendicular to the (101) plane show a non-polar interaction between the inversion-related adjacent phenyl rings of the bupivacaine cations (see Fig. 5). The distance between the least-squares planes through the adjacent phenyl rings is only 3·08 Å. Adjacent layers are held together by van der Waals contacts.

Molecular modelling

The use of orientation and translation searches (*e.g.* as implemented in the *DIRDIF* system) necessitates a

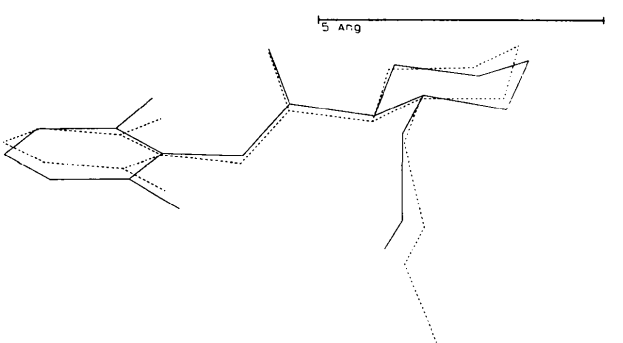

Fig. 3. Stick drawing of the ropivacaine and bupivacaine cations (non-H atoms only) showing their similar overall conformations. Least-squares fit of all common non-H atoms: mean deviation = 0·22 Å. Solid lines, ropivacaine; dashed lines, bupivacaine.

model of part of the structure of interest. It has been shown (Parthasarathi, Beurskens & Bruins Slot, 1983) that the size of the model should constitute at least 10% of the total scattering power and that errors in the atomic positions of the model up to 0·3 Å are acceptable for a successful application of *DIRDIF*. The result of a search of the CSD, where a rigid part of the structure is extracted, is normally used as input. However, given the rather large acceptable error, the use of molecular-modelling programs to get *a priori* structural information for the X-ray structure determination process should be considered as a viable alternative. To be applicable, two conditions have to be satisfied: the model may only contain atoms for which parameters are available in the molecular-modelling program; and from a practical point of view, the number of degrees of freedom should be limited. In the present study both crystal structures were solved using the fragment (I), the coordinates of which were obtained from molecular-mechanics calculations as implemented in *MacroModel* (Mohamadi *et al.*, 1990). The models have a scattering power of about 30 and 15% of the total scattering power of ropivacaine and bupivacaine, respectively. After the structure determination process, the mean deviations between the atomic positions in the model and the final positions of the corresponding atoms in the crystal structures are 0·118 and 0·236 Å, respectively. Because the model contains only two degrees of freedom [rotations about C(1)—N(1) and C(9)—C(10)], it is interesting to compare the predicted results from various modelling programs as well as those from semi-empirical MO calculations.

Table 5. *Distances* (Å) *and angles* (°) *involved in hydrogen bonding for ropivacaine and bupivacaine*

	D···*A*	*D*—H	H···*A*	*D*—H···*A*
Ropivacaine				
N(2)···Cl(1)	3·107 (3)			
O(2)···Cl(1)	3·109 (4)			
N(2)···O(1)	2·836 (4)			
O(2)···O(1)	2·838 (4)			
N(1)—H(1)···O(2^{i})	2·910 (5)	0·82 (5)	2·09 (5)	175 (4)
Bupivacaine				
N(1)—H(1)···Cl(1)	3·183 (3)	0·84 (4)	2·35 (4)	173 (4)
N(2)—H(2)···O(1)	2·771 (4)	0·83 (4)	2·58 (4)	94 (4)
N(2^{ii})—H(2^{ii})···Cl(1)	3·100 (3)	0·83 (4)	2·32 (4)	156 (4)
O(20^{ii})···Cl(1)	3·321 (17)			
O(21^{iii})···Cl(1)	3·291 (19)			

Symmetry code: (i) $x, y+1, z$; (ii) $-x+\frac{3}{2}, y-\frac{1}{2}, -z+\frac{3}{2}$; (iii) $x+\frac{1}{2}, -y-\frac{1}{2}, z-\frac{1}{2}$.

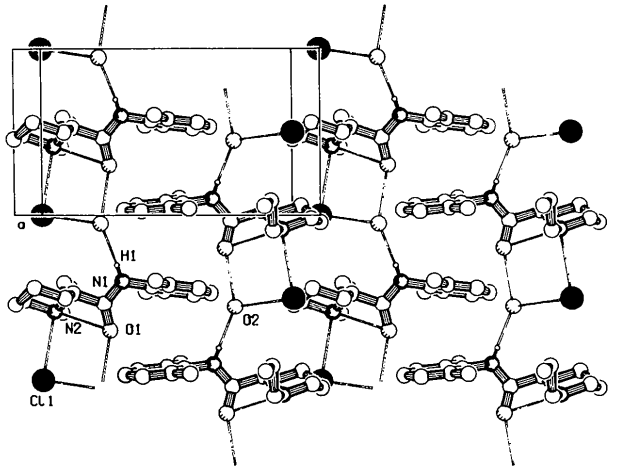

Fig. 4. Hydrogen-bonded chains in ropivacaine, viewed perpendicular to the *bc* plane.

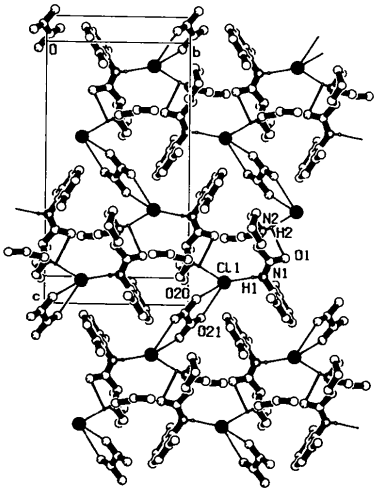

Fig. 5. Hydrogen-bonding scheme in bupivacaine, viewed perpendicular to the *bc* plane.

MacroModel

In addition to straightforward molecular-mechanics calculations, to obtain the model for structure determination from a sketched fragment, *MacroModel* (see *e.g.* Mohamadi *et al.*, 1990) was also used for a multiconformer analysis of the model (a procedure to minimize the risk of missing the global minimum-energy conformation). Multiple conformations were generated using the *MULTIC* (Lipton & Still, 1988) option in *MacroModel*. Characteristics for this calculation and the ensuing minimizations are summarized in Table 6. Energy minimization, in which duplicate conformations are removed, converged to eight structures. These eight conformations occur as four identical pairs, because of the topological symmetry of the dimethylphenyl group. Fig. 6 shows the four unique conformations together with the non-hydrogen skeleton of ropivacaine. The results were analyzed using *GSTAT*89 (Cambridge Crystallographic Data Centre, 1989) and *CHEMX* (Chemical Design Ltd, 1988). It appears

Table 6. *MacroModel multiconformer analysis*

Generation of conformers
Number of rotations: 2
Rotation 1: N(2)—C(10)—C(9)—N(1); 12 values: −150, 180, 30°
Rotation 2: C(11)—N(1)—C(1)—C(2); 12 values: −150, 180, 30°

Non-bonded distance cutoff = 1·5 Å
Heavy-atom 1,5 distance cutoff = 3·0 Å
Max. number of bad 1,5 interactions allowed = 99
Number of interatomic distance constraints = 0

Number of conformations generated = 70
Total energy used in calculations
Minimum energy: 89·5 kJ mol^{-1}
Maximum energy: 171·6 kJ mol^{-1}

Minimization of conformers
300–350 cycles block-diagonal Newton–Raphson using *AMBER*
Hydrogen addition after 200–250 cycles BDNR
Minimum energy: 27·65 kJ mol^{-1}
Maximum energy: 51·78 kJ mol^{-1}
Averaged first derivative r.m.s.: 0·21 kJ Å^{-1}
Unique conformations:

Number	Energy (kJ mol^{-1})	R.m.s. (kJ Å^{-1})	C(2)—C(1)—N(1)—C(9) (°)	N(1)—C(9)—C(10)—N(2) (°)
1	27·65	0·36	−129·73	157·31
2	29·34	0·17	−51·71	152·08
3	50·04	0·18	−52·60	−100·86
4	50·60	0·23	−129·29	−94·73

that the global minimum-energy structure (conformation 1) is close to the conformation of ropivacaine and of bupivacaine. The average error in the geometry of this conformation compared to the moieties in ropivacaine and bupivacaine is summarized in Table 7.

An alternative way to search the conformational space is the minimization of multiple conformations using constraints. *MacroModel* was applied to generate conformations with assigned torsion-angle values of $0 + n \times 30°$ for C(2)—C(1)—N(1)—C(9) (n = 0...6) and N(1)—C(9)—C(10)—N(2) (n = 0...11), comprising a set of 84 conformations. These conformations were minimized using the *AMBER* force field (as implemented in *MacroModel*) in the all-atom approach using constraint force constants of

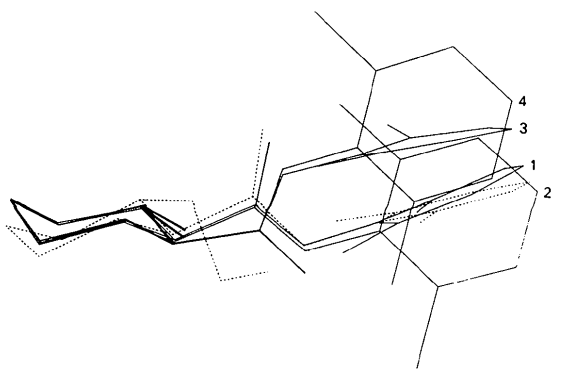

Fig. 6. *MacroModel MULTIC* results as compared with the crystal structure of ropivacaine. A superimposition of the piperidine fragments of the *MULTIC* results together with a superimposition of the common non-H atoms of ropivacaine with *MULTIC* result (1). Relative energies (kJ mol^{-1}): (1) 27·65, (2) 29·34, (3) 50·04, (4) 50·60. Dashed lines: ropivacaine.

Table 7. *Averaged geometric differences of lowest energy conformation obtained from MacroModel MULTIC mode compared to ropivacaine and bupivacaine*

	Ropivacaine	Bupivacaine
Deviations from least-squares fit (Å)	0·28	0·16
Mean absolute difference in		
Bond lengths (Å)	0·017 (13)	0·018 (11)
Valence angles (°)	1·8 (12)	1·2 (11)
Torsion angles (°)	9 (7)	9 (7)
Maximum absolute difference in		
Bond lengths (Å)	0·052 [C(1)—N(1)]	0·045 [C(1)—N(1)]
Valence angles (°)	3·8 [C(10)—N(2)—C(14)]	3·6 [C(14)—N(2)—C(15)]
Torsion angles (°)	27·9 [C(6)—C(1)—N(1)—C(9)]	25·9 [C(6)—C(1)—N(1)—C(9)]

1000 kJ ($V1 = -1000$ kJ) for the preset torsion angles C(2)—C(1)—N(1)—C(9) and N(1)—C(9)—C(10)—N(2). The results are depicted in Fig. 7, in which the relative energies (kJ mol^{-1}) are mapped as a function of the constrained torsion angles.

In this contour plot the conformation of ropivacaine as found from the X-ray analysis and the conformations of the model obtained from the application of the *MacroModel MULTIC* mode are highlighted. From this contour plot it is clear that, in this particular case, results from the multiconformer analysis and the constraint minimizations are almost

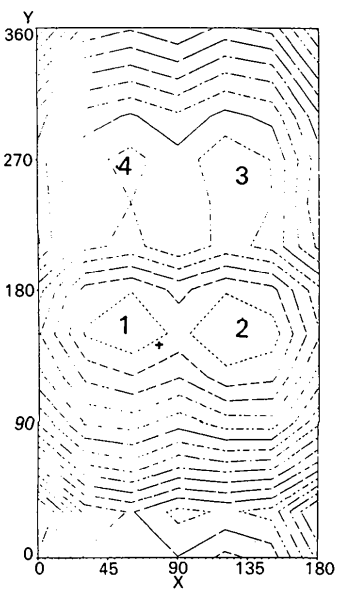

Fig. 7. *MacroModel* constraint energy minimization results (relative energies with 5 kJ mol^{-1} contour levels) as function of torsion angles C(2)—C(1)—N(1)—C(9) (x axis) and N(1)—C(9)—C(10)—N(2) (y axis). + denotes the ropivacaine crystal structure, 1–4 denote the *MacroModel MULTIC* conformations.

identical. With the multiconformer analysis all minimum energy conformations are found, but no estimates of the energy barriers for rotation about C(1)—N(1) and C(9)—C(10) can be obtained as is possible with the constraint minimizations. The variation of the energy for constant values of torsion angle N(1)—C(9)—C(10)—N(2) (any horizontal line in Fig. 7) is much smaller than the variation of the energy for constant values of torsion angle C(2)—C(1)—N(1)—C(9) (any vertical line in Fig. 7). Thus, the torsion angle around C(1)—N(1) will be less accurately defined by *MacroModel* than the torsion angle around C(9)—C(10). This is illustrated by the results from the multiconformer analysis, where the lowest energy conformation (see Table 7) differs by 26·6° in torsion angle C(2)—C(1)—N(1)—C(9) and by only 14·4° in torsion angle N(1)—C(9)—C(10)—N(2) from the crystal structure results for ropivacaine. Compared to bupivacaine, these differences are 25·4 and 14·3°, respectively.

Biograf

The results of constraint minimizations using *Biograf* (BioDesign Inc., 1989) with the Dreiding force field (Mayo, Olafson & Goddard, 1989) are depicted as a contour plot in Fig. 8. Torsion angles C(2)—C(1)—N(1)—C(9) and N(1)—C(9)—C(10)—N(2) were constrained at the above mentioned values using a constraint force constant of 837 kJ, and minimizations were carried out using the conjugate gradient method until the residual total force was less than 0·42 kJ mol^{-1} Å^{-1}. The overall energy surface is comparable with the results of the constraint minimization using *MacroModel*. The torsion angles of the low-energy conformation predicted by *Biograf* differ by about 45 and 20° for C(2)—C(1)—N(1)—C(9) and N(1)—C(9)—C(10)—N(2), respectively, as compared with the crystal structure of ropivacaine.

Semi-empirical MO calculations

The results for the analysis of the conformational space using *VAMP* (1989), a vectorized molecular orbital package, are quite remarkable. As in the constraint minimizations using *MacroModel* and *Biograf*, conformations were generated with torsion angles C(2)—C(1)—N(1)—C(9) and N(1)—C(9)—C(10)—N(2) set to $0 + n \times 30°$. The different conformations were fully optimized, 'constraining' the aforementioned torsion angles. The heats of formation as a function of both unoptimized torsion angles are given in Fig. 9. [Because of the time-consuming processes involved, only the conformations with torsion angle C(2)—C(1)—N(1)—C(9) varying from 0–90° were optimized, since no considerable differences in energies were found for the complementary part of the energy surface from *MacroModel* or from *Biograf*]. Although the conformation of the model as found in ropivacaine by X-ray analysis is within a low-energy region, no distinct set of torsion angles for low-energy conformations can be deduced from the calculations. A

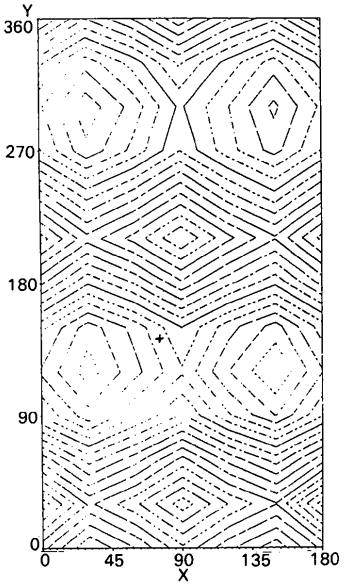

Fig. 8. *Biograf* constraint energy minimization results (relative energies with 5 kJ mol^{-1} contour levels) as function of torsion angles C(2)—C(1)—N(1)—C(9) (x axis) and N(1)—C(9)—C(10)—N(2) (y axis). + denotes the ropivacaine crystal structure.

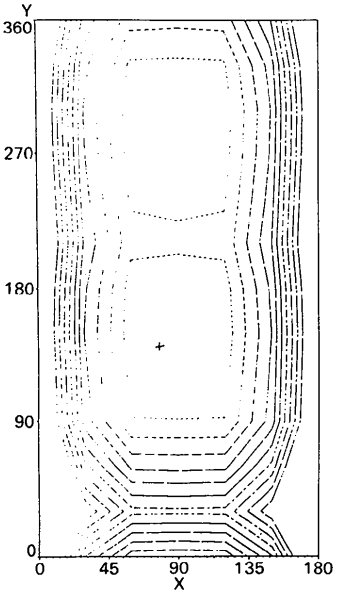

Fig. 9. *VAMP* results (relative energies with 10 kJ mol^{-1} contour levels) as function of torsion angles C(2)—C(1)—N(1)—C(9) (x axis) and N(1)—C(9)—C(10)—N(2) (y axis). For comparison with Figs. 8 and 9, the results were extrapolated for $90 < x < 180°$. + denotes the ropivacaine crystal structure.

prediction of the conformation from *VAMP* optimizations to serve as a starting model for the structure determination would be an unacceptable approximation.

Concluding remarks

Ropivacaine and bupivacaine crystallize in the same conformation, although their crystallographic packing schemes are quite different. This conformation of the active (protonated) form of both molecules was recognized earlier (Yoo *et al.*, 1975) in related lidocaine derivatives. Molecular-mechanics calculations as implemented in *MacroModel* and *Biograf* can be used to predict these conformations relatively accurately, in contrast to the semi-empirical molecular-orbital calculations.

We are grateful to Dr Jan Noordik for valuable discussions, and we thank Dr Jos Lange for preparing the crystals and Drs José van der Mijden for her assitance during the crystal structure determinations. Use of the services and facilities of the Dutch CAOS/CAMM Center, under grant Nos. SON-326-052 and STW-NCH99.1751, is gratefully acknowledged.

References

ALLEN, F. H., BELLARD, S., BRICE, M. D., CARTWRIGHT, B. A., DOUBLEDAY, A., HIGGS, H., HUMMELINK, T., HUMMELINK-PETERS, B. G., KENNARD, O., MOTHERWELL, W. D. S., RODGERS, J. R. & WATSON, D. G. (1979). *Acta Cryst.* B**35**, 2331–2339.

BEURSKENS, G., NOORDIK, J. H. & BEURSKENS, P. T. (1980). *Cryst. Struct. Commun.* **9**, 23–28.

BEURSKENS, P. T., BOSMAN, W. P., DOESBURG, H. M., GOULD, R. O., VAN DEN HARK, TH. E. M., PRICK, P. A. J., NOORDIK, J. H., BEURSKENS, G., PARTHASARATHI, V., BRUINS SLOT, H. J. & HALTIWANGER, R. C. (1984). *DIRDIF*. Tech. Rep. 1984/1. Crystallography Laboratory, Univ. of Nijmegen, The Netherlands.

BEURSKENS, P. T., GOULD, R. O., BRUINS SLOT, H. J. & BOSMAN, W. P. (1987). *Z. Kristallogr.* **179**, 127–159.

BioDesign Inc. (1989). *Biograf*. Molecular modelling software. BioDesign Inc., Pasadena, USA.

Cambridge Crystallographic Data Centre (1989). *GSTAT*89. Numerical calculations package for structures retrieved from the CSD. In *CSD Users Manual*. Cambridge Crystallographic Data Centre, Cambridge, England.

Chemical Design Ltd (1988). *ChemX*. Molecular modelling software. Chemical Design Ltd, Oxford, England.

FAGGIANI, R., LOCK, C. J. L., DEUTSCH, E., RICHARDS, P. & SRIVASTAVA, S. C. (1982). *Acta Cryst.* B**38**, 733–736.

GERMAIN, G., DECLERCQ, J.-P., VAN MEERSSCHE, M. & KOCH, M. H. J. (1977). *Acta Cryst.* B**33**, 1971–1972.

GŁOWKA, M. L. & GAŁDECKI, Z. (1981). *Pol. J. Chem.* **55**, 651.

GRANT, D. F. & GABE, E. J. (1978). *J. Appl. Cryst.* **11**, 114–120.

HANSON, A. W. (1972). *Acta Cryst.* B**28**, 672–679.

HANSON, A. W. & BANNER, D. W. (1974). *Acta Cryst.* B**30**, 2486–2488.

HANSON, A. W. & ROHRL, M. (1972). *Acta Cryst.* B**28**, 3567–3571.

KLYNE, W. & PRELOG, V. (1960). *Experientia*, **16**, 521–523.

LEHMAN, M. S. & LARSEN, F. K. (1974). *Acta Cryst.* A**30**, 580–584.

LIPTON, M. & STILL, C. W. (1988). *J. Comput. Chem.* **9**, 343–355.

MAYO, S. L., OLAFSON, B. D. & GODDARD, W. A. III (1989). *Biograf Reference Manual*, Version 2.0, pp. L1 – L10. BioDesign Inc., Pasadena, USA.

MOHAMADI, F., RICHARDS, N. G. J., GUIDA, W. C., LISKAMP, R., LIPTON, M., CANFIELD, C., CHANG, G., HENDRICKSON, T. & STILL, W. C. (1990). *J. Comput. Chem.* **11**, 440–467.

NARDELLI, M. (1983). *Comput. Chem.* **7**, 95–98.

NORTH, A. C. T., PHILLIPS, D. C. & MATHEWS, F. S. (1968). *Acta Cryst.* A**24**, 351–359.

PARTHASARATHI, V., BEURSKENS, P. T. & BRUINS SLOT, H. J. (1983). *Acta Cryst.* A**39**, 860–864.

SHELDRICK, G. M. (1976). *SHELX*76. Program for crystal structure determination. Univ. of Cambridge, England.

SPEK, A. L. (1982). *The EUCLID Package*. In *Computational Crystallography*, edited by D. SAYRE, p. 528. Oxford: Clarendon Press.

VAMP (1989). Vectorized molecular orbital package. Version 4.10. (Based on *AMPAC*1.0 and *MOPAC*4.0). Univ. of Erlangen, Federal Republic of Germany.

WALKER, N. & STEWART, D. (1983). *Acta Cryst.* A**39**, 158–166.

YOO, C. S., ABOLA, E., WOOD, M. K., SAX, M. & PLETCHER, J. (1975). *Acta Cryst.* B**31**, 1354–1360.

Acta Cryst. (1990). B**46**, 850–854

Deformation-Density Studies of Thiathiophthenes. I. 2,5-Dimethyl-6a-thiathiophthene

BY YU WANG,* S. Y. WU AND A. C. CHENG

Department of Chemistry, National Taiwan University, Taipei, Taiwan

(*Received* 21 *May* 1990; *accepted* 16 *July* 1990)

Abstract

The title compound, 2,5-dimethyl[1,2]dithiolo[1,5-*b*]-[1,2]dithiole-7-S^{IV}, $C_7H_8S_3$, was studied by X-ray diffraction at both 110 and 300 K. Space group *Pnma*, $Z = 4$, $M_r = 188{\cdot}32$, $a = 7{\cdot}956\ (4)$, $b = 19{\cdot}920\ (7)$, $c = 5{\cdot}361\ (2)$ Å, $V = 811{\cdot}4\ (6)$ Å^3 at 110 K. Mo $K\alpha$ radiation ($\lambda = 0{\cdot}7107$ Å, $\mu = 0{\cdot}80$ mm^{-1}), $R = 0{\cdot}036$ and $0{\cdot}032$ for 1527 and 449 reflections at 110 and 300 K respectively. The crystal structures are the same at both temperatures. The

* To whom all correspondence should be addressed.

0108-7681/90/060850-05$03.00